International Journal of Scientific Engineering and Research (IJSER)
ISSN (Online): 2347-3878
SJIF (2024): 6.623

Design and Development of a Real-Time Displacement Monitoring System for Structures Using GNSS Technology

Khai Cong Pham

Hanoi University of Mining and Geology, No.18 Vien Street - Duc Thang Ward- Bac Tu Liem District - Ha Noi
Email: *khaingocthuy2002[at]gmail.com*

Abstract: ***This article presents the design and development of a real-time displacement monitoring system for structures using GNSS/CORS technology. The proposed system comprises three key components: a CORS station, a monitoring station, and a data transmission unit. The CORS station employs the Nets9 GNSS receiver, while the monitoring station integrates a receiver developed using the Trimble BD970 module. Real-time data are transmitted via the internet using the NTRIP protocol and processed in NMEA format. A sliding window algorithm is implemented to detect displacements, and the system's performance was validated through simulation experiments. Results demonstrated high accuracy, with maximum differences of 5 mm horizontally and 8 mm vertically when compared with laser distance meter readings.***

Keywords: GNSS; CORS; RTK; displacement monitoring; sliding window algorithm

1. Introduction

The industrialization and urbanization processes are occur quickly during the last several decades which lead to industrial and civil construction projects are getting bigger and higher. However, the construction works on the ground are often displaced and deformed due to the impact of many different factors, therefore, monitoring displacement and deformation of construction works is an important task. The real time identification of the deformation and displacement of buildings can reduce the risk of accidents that can happen to people and avoid financial losses. Up to now in Vietnam most of the deformation and displacement monitoring works are mainly periodically carried out by traditional measuring devices such as hydrography, theodolite, electronic total or by GPS technology. Using this technology and equipments it is difficult to real time monitor continuously changing deformation and displacement.

The deformation and displacement surveying need to be automatically and continuously carried out in real time due to the rapid development of new technology. The deformation and displacement surveying of high-rise buildings has been effectively studied by GNSS technology [1], [2]. Deflection and horizontal displacement of bridges can be determined by using GNSS technology [3]. The GNSS system currently allows the continuously reception of satellite signals using real-time RTK dynamic measurement technology with high accuracy. The advantages of GNSS technology are to provide 3D data in real time, operate continuously with different weather conditions, position with high precision; therefore, this technology has been applied to survey effectively spherical displacement and deformation [4]. The aim of this study is to design and develop a real-time displacement and deformation monitoring system for civil structures using GNSS/CORS technology.

GNSS technology monitoring system has been widely and effectively applied in many countries over the world. However, these systems all have their own hardware, software and high cost. Therefore, the idea of developing a system for real time continuously monitoring deformation transformation based on GNSS/CORS technology has been proposed. Based on the working principle and data transmission mechanism of CORS station, this work has developed a device to receive and transmit the corrected data from the user (User) located at the monitoring position to master station (Server). All measurements from the used station are automatically and continuously sent to the master station. Here a software has been designed to handle the measured data that was sent from user at the monitoring point to produce the results of the immediately displacement and deformation of the construction works. To test the accuracy and stability of the system, a dedicated device has been designed and manufactured. The experiments data show that the monitoring system works properly, stably, continuously 24/7 and can monitor the deformation and displacement of the construction works from 3 mm upwards. This study is significant as it offers a cost-effective and high-precision alternative to conventional displacement monitoring methods, enabling continuous and automated structural surveillance critical for public safety and asset protection.

2. Methods

2.1 Design of the GNSS-based Displacement Monitoring System

The GNSS-based displacement monitoring system of works in real-time must be designed to ensure stable and continuous operation, signal decoding, data transmission, processing, and real-time display. The system consists of three main components shown in Figure 1; the first component is the single CORS station, the second component is the network of monitoring stations, and the third component is the data transmission system

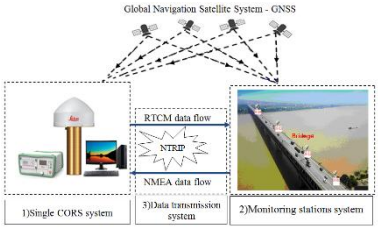

Figure 1: Diagram of the displacement monitoring system of works based on single CORS technology

The single CORS system provides positional correction to the monitoring stations in the standard Radio Technical Commission for Maritime Services (RTCM) format. It processes the data of RTK measurement networks, corrects integer ambiguities of the CORS system, and develops correction models for tropospheric, ionospheric, and satellite orbit errors. Additionally, the CORS station's main computer hosts the data processing software for the CORS station, monitoring data processing software, and serves as a data storage center. The monitoring station system consists of multiple GNSS receivers working based on the RTK relative method. The GNSS receivers connect with the CORS station's main computer via a 4G WiFi modem and receive positional corrections from the CORS station to obtain accurate coordinates. The corrected coordinates of the monitoring stations are transmitted to the main computer in the standard NMEA format [5].

The data transmission system is responsible for transmitting positional corrections from the CORS station to the monitoring stations, and transmitting the data from the monitoring stations to the main computer of the CORS station. Data transmission is carried out using the Network Transport of RTCM via Internet Protocol (NTRIP) protocol [6]. The monitoring system operates based on the GNSS relative positioning method, utilizing carrier-phase combined with pseudorange measurements. To eliminate or minimize certain error sources affecting positioning results, differencing equations (phase differences) are employed. The second-order differencing equations of the CORS station, the monitoring station, and two satellites i and j eliminate satellite and receiver clock errors and, therefore are commonly used to determine the baseline vector. The second-order differencing equations for pseudorange and carrier-phase measurements are [7]:

$$\left.\begin{aligned} \Delta\nabla P_{MC}^{i,j} &= \Delta\nabla\rho_{MC}^{i,j} + \Delta\nabla I_{MC}^{i,j} + \Delta\nabla T_{MC}^{i,j} + \Delta\nabla\varepsilon_P \\ \lambda.\Delta\nabla\phi_{MC}^{i,j} &= \Delta\nabla\rho_{MC}^{i,j} - \Delta\nabla I_{MC}^{i,j} + \Delta\nabla T_{MC}^{i,j} - \lambda.\Delta\nabla N_{MC}^{i,j} + \Delta\nabla\varepsilon_\phi \end{aligned}\right\} \quad (1)$$

Where $\Delta\nabla$ is the second-order difference, i and j are the non-reference and the reference satellites, M and C are the monitoring and the CORS stations, P and ϕ are the pseudorange and the carrier-phase measurements, λ is the carrier wavelength, ρ is the geometric distance between the monitoring and CORS stations to the satellites, I is the ionospheric delay, T is the tropospheric delay, N is the integer ambiguity, εP is the random pseudorange noise and other errors.

Additionally, in relative positioning, it is necessary to minimize errors caused by tropospheric and ionospheric delays. These errors have a spatial correlation with the baseline length; therefore, to reduce their impact on RTK positioning, the baseline length should not exceed 10 km.

2.2. Establishment of the CORS Station System

The main components of a CORS station are the GNSS CORS antenna and receiver. In addition, there are several auxiliary components, such as data transmission cables, internet connection and modem, server computer, power supply, and uninterruptible power supply (UPS).

1) GNSS CORS antenna

The antenna used in the CORS station must be designed to ensure high phase center stability, eliminate multipath errors, improve measurement accuracy, and provide the best positioning solutions by receiving satellite signals within the GNSS system. In this study, we use a Choke-ring antenna of South company (China).

2) GNSS CORS receiver

The GNSS receiver used in the CORS station is the NetS9 receiver of South company (China), The NetS9 receiver offers high accuracy, robust performance, and stability. It can receive signals from 440 channels of satellites in the GNSS constellation, determine coordinates using carrier-phase measurements with an accuracy of less than 1mm, and support data linking through 4G telecommunication networks, Bluetooth, and WLAN. It can be easily configured via WebUI and remote computers and supports the NTRIP server and NTRIP Caster. The accuracy for static measurements is 3mm+0.1ppm in the horizontal and 3.5mm+0.4ppm in the vertical. The accuracy for RTK measurements is 8mm+1ppm in the horizontal and 15mm+1ppm in the vertical [8].

The GNSS antenna is installed on a pillar that has been surveyed and selected in accordance with technical standards, ensuring it is securely and stably constructed. The GNSS CORS antenna is located in Hanoi University of Mining and Geology, Vietnam. The CORS station has the identifier N001.

2.3 Determination of the coordinates of the CORS station

The coordinates of the N001 station are adjusted using the Bernese 5.2 software and connected to several nearby IGS stations in the area The input data in the Rinex format used in the adjustment are obtained from the CORS station over an observation duration of 48 hours.

The coordinates of the CORS station N001 after adjustment in the geocentric Cartesian coordinate system and their root mean square error are shown in Table 1.

The coordinates of the N001 station are input to the GNSS NetS9 receiver via the WebUI (User Interface) by logging into the receiver through the Internet Explorer browser and entering the IP address.

2.4 Design of the components of the real-time monitoring system

The components of the real-time displacement monitoring system we designed are shown in Figure 2.

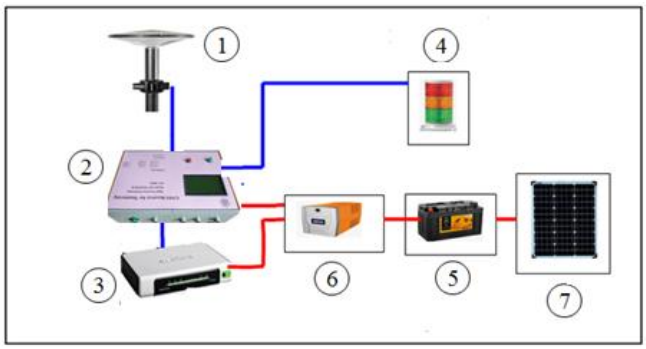

Figure 2: Components of the real-time displacement monitoring station system: (1) GNSS antenna; (2) GNSS receiver; (3) WiFi modem with 4G sim card; (4) Alarm and signaling module; (5) 12V battery; (6) Solar energy-charged controller; (7) Solar panel

Table 1: Geocentric Cartesian coordinates of CORS stations after adjustment

No	Station	Components of the geocentric Cartesian coordinate system (m)			RMSE (m)		
		X	Y	Z	m_X	m_Y	m_Z
1	N001	-1618564.5576	5730005.6206	2278800.1280	0.0002	0.0004	0.0002
2	BJFS	-2148744.3455	4426641.2277	4044655.8698	0.0002	0.0005	0.0003
3	DAEJ	-3120042.2172	4084614.7731	3764026.8438	0.0003	0.0005	0.0004
4	IISC	1337936.1054	6070317.1240	1427877.0782	0.0003	0.0014	0.0040
5	LHAZ	-106941.8237	5549269.8253	3139215.1274	0.0002	0.0007	0.0003
6	NTUS	-1508023.0421	6195576.5830	148799.3612	0.0002	0.0007	0.0002
7	PIMO	-3186293.6975	5286624.3462	1601158.3573	0.0004	0.0006	0.0002
8	SHAO	-2831733.7544	4675665.8461	3275369.3288	0.0002	0.0005	0.0003
9	TCMS	-2982783.1668	4966659.9928	2658809.3788	0.0003	0.0005	0.0003
10	TNML	-2982779.3508	4966662.5248	2658805.6462	0.0003	0.0006	0.0003
11	TWTF	-2994428.4187	4951309.1839	2674496.7141	0.0003	0.0005	0.0003
12	WUHN	-2267749.6867	5009154.2159	3221290.6190	0.0003	0.0007	0.0004

The name and features of each component in the real-time displacement monitoring system of works are shown in Table 2.

Table 2: Name and features of each component in the monitoring system

No	Component	Feature	Note
1	GNSS antenna	Receiving GNSS signal	Supplied by the manufacturer
2	GNSS receiver	Receiving and decoding GNSS signals.	Self-developed
3	WiFi modem with 4G sim card	Transmission of monitoring data	Supplied by the manufacturer
4	Alarm and signaling module	Warning through sounding and lighting.	Supplied by the manufacturer
5	12V battery	Storage and supplying power for the GNSS receiver and modem.	Supplied by the manufacturer
6	Solar energy-charged controller	Charging the battery.	Supplied by the manufacturer
7	Solar panel	Providing input power for the monitoring station system.	Supplied by the manufacturer

2.5 Design and development of the GNSS receiver for the monitoring station

The GNSS receiver is designed and developed based on the Trimble OEM BD970 module. This module can receive 220 channels from satellite systems, such as GPS (L1C/A, L2E, L2C, L5), GLONASS (L1C/A, L1P, L2C/A, L2P), SBAS (L1C/A, L5), Galileo (L1BOC, E5A, E5B, E5AltBOC1), BeiDou (B1, B2), and QZSS (L1C/A, L1 SAIF, L2C, L5). The RTK positioning accuracy is 8mm+1ppm in the horizontal component and 15mm+1ppm in the vertical component, with a baseline of up to 30km [9]. This module has an Ethernet LAN port. It can be connected to a WiFi modem to transmit monitoring data to the server computer via an IP address and access port on the modem at the CORS station. The GNSS BD970 module, combined with other selected modules, is connected and assembled to form a complete GNSS receiver for the monitoring station system as shown in (Figure 3) are the front and behint of the GNSS receiver.

The GNSS receiver operates using a computer program written in the C# programming language within the Arduino software environment. The program source code is uploaded to the Atmega328P control chip of the GNSS receiver via the Arduino UNO module, which is connected to the computer through a USB port.

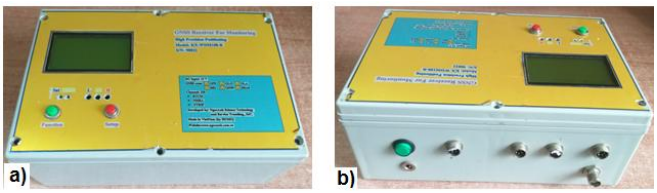

Figure 3: GNSS receiver used in the monitoring station: (a) Front, (b) Behind.

The GNSS receiver, combined with other components, as shown in Table 1, forms the real-time monitoring station system in Figure 4. This monitoring station system performs real-time kinematic (RTK) measurements with high accuracy. It transmits the data to the main computer via an IP address and access port previously configured.

Figure 4: Real-time displacement monitoring system of works

3. Data Processing, Analysis, and Displacement Detection

Data processing, analysis, and displacement detection involve three steps: detection and removal of outliers in the RTK time series, converting geocentric Cartesian coordinates to local topocentric coordinates in the WGS84 reference, and analyzing the data to detect displacement.

3.1 Outlier Detection in RTK Time Series

In continuous monitoring based on GNSS RTK techniques, outliers may appear alongside points of change caused by sudden displacements. Therefore, during data processing, it is necessary to identify and remove outliers from the time series. In Figure 6, points I, II, and III are outliers, while point IV is a point of change (also known as a displacement point). Outliers are due to relatively significant deviations in the time series. In contrast, displacement points are caused by changes in state over time within the time series. As shown in Figure 5, after 11:12:15, a change occurred in the measurement time series, and the displacement point was detected.

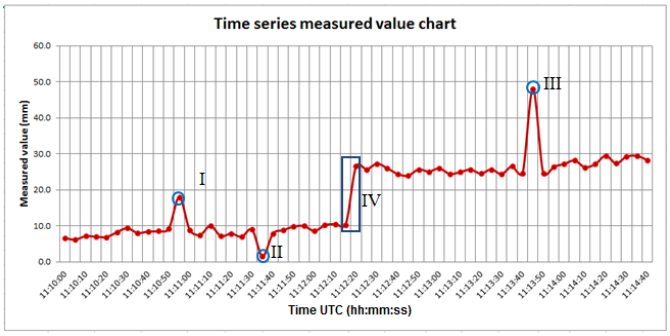

Figure 5: Outlier and displacement points in the time series. I, II, and III are outliers, and IV is the displacement point.

It is challenging to detect and remove outliers in observational data without accompanying information, especially with large datasets. To detect outliers in the measurement time series, this study utilizes observational data in the standard NMEA format. NMEA-standard data includes messages of different types. To reduce the size of observational data and ensure more stable data transmission, we use two types of measurement messages: GGA and GST. These messages contain positional information and other supplementary data, making them suitable for the detection and removal of outliers. The GGA message is the most commonly used in GPS or GNSS positioning. It includes the following information: UTC (1), latitude (2), northing (3), longitude (4), easting (5), a quality indicator of positioning (6), the number of satellites used (7), horizontal dilution of precision (8), antenna height above the geoid (9), a unit of antenna height (10), separation between the WGS-84 ellipsoid and the geoid (11), unit of the baseline in meter (12), age of differential GPS data record (13), ID of the reference station, ranging from 0000 to 4095 (14), and checksum of the message string (15). The structure of a GGA message and its details are shown in Figure 6.

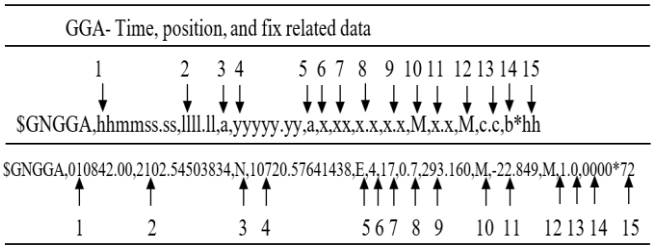

Figure 6: Structure of GGA message and its details

The GST message contains information about the position correction time (1), residuals of pseudo-range (2), semi-major axis of the error ellipse (3), semi-minor axis of the error ellipse (4), orientation angle of the semi-major axis of the error ellipse (5), error in the Y-axis (6), error in the X-axis (7), vertical error (8), and the message string checksum (9). The structure of the GST message and its details are shown in Figure 7.

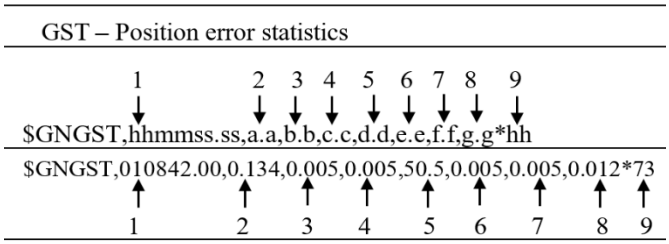

Figure 7: Structure of the GST message and its details

In GGA messages, there is an indicator of the quality of RTK results with six levels numbered from 0 to 5. An indicator of 4 indicates RTK results of high accuracy, and the user will accept this message. Potential outliers are detected based on the following three criteria: completeness of the message series, RTK positioning quality indicator, and the position error. The detection of potential outliers is carried out in the following three steps:

Step 1) Removal of incomplete messages
NMEA-standard messages transmitted from the monitoring station to the central computer via the NTRIP protocol may encounter transmission errors, resulting in incomplete information. To filter out these incomplete messages, their integrity must be verified. If the messages lack complete information, the corresponding measurement data lines are discarded. To verify the integrity of the information in the measurement message series, all characters in the series are analyzed from the "$" character to the "*" character. Then, a bitwise operation algorithm is applied, starting from the first character to the next, until the end of the series, to generate a new parsed checksum. This parsed checksum is then compared with the checksum included in the transmitted message. If the two checksums match, the measurement data line is accepted to proceed to the second filtering step.

Step 2) Filtering of position-corrected measurement messages

In RTK positioning, the measurement quality can vary at different levels, which is reflected in the quality indicator in the GGA message. The RTK measurement quality indicator has six levels numbered from 0 to 5. An indicator of 4 corresponds to RTK positioning of the best quality, and the message is retained. Messages with indicators 0, 1, 2, 3, and 5 will be discarded. The filtering of the messages to derive the best quality observation is done by analyzing the GGA message string as described in Table 3.

Step 3) Filtering of the measurement messages by position errors

The messages with the best quality have been retained after step 2. However, the RTK positioning errors also vary, as shown in the GST message. To achieve high accuracy, only the messages with position errors smaller than the allowed limits will be retained. The filtering of messages by position errors within the allowable limits is carried out by analyzing the GST message string as described in Table 4. In this study, the horizontal and the vertical error limits of 4mm and 8mm are used. In Figure 8, points I, II, and III are outliers, while point IV is the change point (also known as the displacement point). The outliers are caused by relatively significant deviations in the measurement time series. In contrast, the displacement point is due to a sudden change in the position. As shown in Figure 8, after the time 11:12:15, a change occurs in the measurement time series, and the displacement point has been detected.

3.2. Coordinate Conversion

With the established monitoring station system, the RTK) dynamic observation method is used for displacement monitoring. The coordinates of the monitoring station are determined in the geocentric coordinate system with Cartesian components X, Y, Z or geodetic components B, L, H. For convenience in detecting displacement, these coordinate components, after the three steps of noise filtering mentioned above, will be converted into the local tangent plane coordinate system N, E, U. The relationship between the geocentric Cartesian coordinates and the local tangent plane coordinates is:

$$\begin{bmatrix} N_i \\ E_i \\ U_i \end{bmatrix} = R^T . \begin{bmatrix} X_i - X_o \\ Y_i - Y_o \\ Z_i - Z_o \end{bmatrix} \quad (1)$$

where R^T is the rotation matrix determined as:

$$R^T = \begin{bmatrix} -\sin B_0.\cos L_0 & -\sin B_0.\sin L_0 & \cos B_0 \\ -\sin L_0 & \cos L_0 & 0 \\ \cos B_0.\cos L_0 & \cos B_0.\sin L_0 & \sin B_0 \end{bmatrix} \quad (2)$$

where B_0, L_0, H_0 are the geodetic coordinates of the origin point of the local tangent plane coordinate system, X_0, Y_0, Z_0 are the geocentric Cartesian coordinates of the origin point calculated as:

$$\left.\begin{aligned} X_0 &= (N_0 + H_0).cosB_{0-}.cosL_0 \\ Y_0 &= (N_0 + H_0).cosB_{0-}.sinL_0 \\ Z_0 &= \left[N_0(1 - e^2) + H_0\right].sinB_{0-} \end{aligned}\right\} \quad (3)$$

For convenience in developing a computer program, the coordinates of the observation point in the local tangent plane coordinate system can be calculated from Equation (2) using Equation (4) as:

$$\left.\begin{aligned} N_i &= -(X_i - X_0)sinB_0cosL_0 - (Y_i - Y_0).sinB_0sinL_0 + (Z_i - Z_0)cosB_0 \\ E_i &= -(X_i - X_0)sinL_0 + (Y_i - Y_0).sinL_0 \\ U_i &= (X_i - X_0)cosB_0cosL_0 + (Y_i - Y_0).cosB_0sinL_0 + (Z_i - Z_0)sinB_0 \end{aligned}\right\} \quad (4)$$

The horizontal and vertical position time series (Ni, E_i, Ui) of the observation points are analyzed to detect the horizontal and vertical displacement.

3.3 Displacement Detection

Real-time displacement detection identifies the time in which the displacement occurs and estimates its magnitude. In this study, we apply the sliding window (SW) model to detect displacement. The SW model is developed based on the Bayesian equation [10] and is interpreted as follows:

Suppose there is a continuous coordinate time series X(x_1, x_2, …,x_n) corresponding to measurement times T(t_1, t_2, …, t_n), referred to as a large array (large window). First, the coordinates time series is split into several smaller arrays (smaller windows) with adjacent sizes typically chosen as $s \geq 5$ depending on the size of the large window. Specifically, the first window starts from the first coordinate to the s^{th} coordinate; the second window starts from the second coordinate to the $(s+1)^{th}$ coordinate, and this continues until the end of the X array. This approach is called the sliding window method as shown in Figure 8.

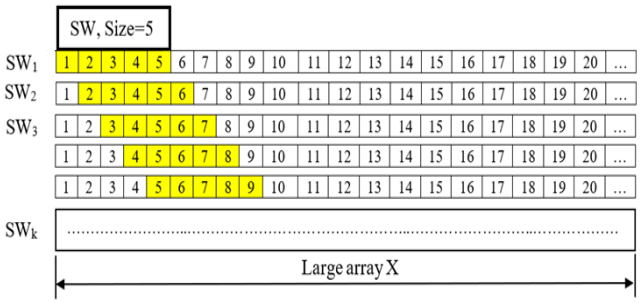

Figure 8: Describe the sliding window method

The sliding window method is based on the variation of the standard deviations of the small window (sub-array) within the large window (main array) of coordinates [11]. Since outliers have been removed previously from the coordinate time series, only displacement points remain. In Figure 8, there are both outliers and displacement points; after outlier removal, only displacement points remain (Figure 9).

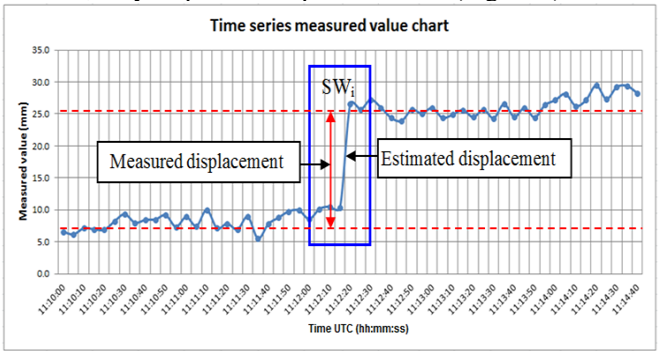

Figure 9: Displacement points in a coordinates time series after outlier removal

After selecting the size of the sliding window, the standard deviation of the i[th] window is computed as [12]:

$$\sigma_i = \sqrt{\frac{\sum_{j=1}^{n}(x_j - \overline{x_i})^2}{s-1}} \quad (5)$$

where x_j is the j[th] observation, i is the sliding window index, $\overline{x_i}$ is the mean value in the i[th] window, s is the window size.

To detect the displacement points, a threshold value of 3σ is used [13]. This threshold is used as:

$$\left|x_j - \overline{x_i}\right| \le 3\sigma \rightarrow Non-displacement\ x_j\ po\text{int}$$

$$\left|x_j - \overline{x_i}\right| \ge 3\sigma \rightarrow Displacement\ x_j\ po\text{int}$$

The estimated displacement value will be calculated as the difference between the measurement value of the last point and its preceding point in the sliding window in which the displacement occurs:

$$Q_{est} = x_j - x_{j-1} \quad (6)$$

Actual displacement value is:

$$Q_m = \frac{1}{n_2}\sum_{k=n_1+1}^{n_2} x_k - \frac{1}{n_1}\sum_{i=1}^{n_1} x_i \quad (7)$$

4. Results and Discussions

4.1 Simulation experimental results

A displacement simulation device is designed and fabricated to verify the feasibility, performance, and accuracy of the proposed monitoring system. The simulation device system, shown in Figure 10, consists of two steel cylindrical tubes of different diameters nested inside each other and positioned vertically. The larger steel tube is fixed, while the smaller steel tube can move vertically inside the larger steel tube to create simulated vertical displacement. A steel circular plate is attached to the top of the smaller steel tube, with a small hole at the center for mounting the GNSS antenna. The smaller steel tube is held in place within the larger steel tube by three locking pins. A metal plate with four small wheels is fixed at the bottom of the larger steel tube. These wheels can move along two horizontal steel bars to create simulated horizontal displacements. A SINCON SD-120C laser distance meter is placed at two fixed reference points to measure horizontal and vertical displacements of the simulation device with an accuracy of ±1mm.

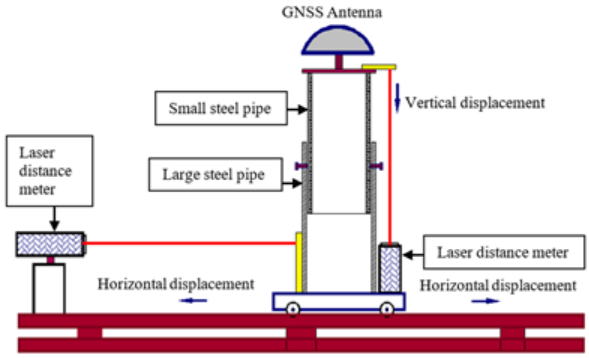

Figure 10: Simulation device used in displacement monitoring: (a) schematic model and detailing parts; (b) real model

a simulation surveying campaigns were conducted in Hanoi City, is shown in Figure 11. The simulation experiments were carried out with both horizontal and vertical displacements. The GNSS antenna was mounted on the simulation device and connected to the GNSS receiver, implementing the RTK positioning method with the CORS N001 station via its IP address and access port. In this experiment, five observation cycles were conducted to create four sudden displacements with random values.

Table 3: Segment of simulated experimental observation data in the standard NMEA format

```
$GNGGA,045806.00,2102.37433863,N,10720.00565021,E,4,29,0.5,253.311,M,-22.879,M,1.0,0000*78
$GNGST,045806.00,0.256,0.011,0.008,140.2,0.010,0.010,0.037*4C
$GNGGA,045807.00,2102.37433986,N,10720.00564929,E,4,29,0.5,253.303,M,-22.879,M,1.0,0000*70
$GNGST,045807.00,0.256,0.011,0.008,140.1,0.010,0.010,0.037*4E
$GNGGA,045808.00,2102.37433966,N,10720.00565108,E,4,29,0.5,253.306,M,-22.879,M,1.0,0000*7E
$GNGST,045808.00,0.257,0.011,0.008,139.6,0.010,0.010,0.037*49
$GNGGA,045809.00,2102.37433900,N,10720.00565052,E,4,29,0.5,253.309,M,-22.879,M,1.0,0000*7E
$GNGST,045809.00,0.256,0.011,0.008,139.4,0.010,0.010,0.037*4B
$GNGGA,045810.00,2102.37433959,N,10720.00565157,E,4,29,0.5,253.312,M,-22.879,M,1.0,0000*74
$GNGST,045810.00,0.257,0.011,0.008,139.6,0.010,0.010,0.037*40
$GNGGA,045811.00,2102.37433920,N,10720.00565074,E,4,29,0.5,253.312,M,-22.879,M,1.0,0000*7B
$GNGST,045811.00,0.257,0.011,0.008,138.8,0.010,0.010,0.038*41
$GNGGA,045812.00,2102.37433921,N,10720.00565097,E,4,29,0.5,253.308,M,-22.879,M,1.0,0000*7F
$GNGST,045812.00,0.257,0.011,0.008,138.2,0.010,0.010,0.038*48
$GNGGA,045813.00,2102.37433946,N,10720.00564967,E,4,29,0.5,253.310,M,-22.879,M,1.0,0000*71
$GNGST,045813.00,0.256,0.011,0.008,139.1,0.010,0.010,0.038*4A
.....
```

Each observation was made during a period of approximately 20 minutes, with a signal interval or sampling rate of 5 seconds. After each observation cycle, the antenna's position was changed horizontally and vertically to create simulated displacements. The differences in horizontal and vertical distances from the reference point of the laser distance meter to the antenna's phase center were considered the displacement magnitudes.

Figure 11: Study area of real-time displacement simulation in the Google Earth map

Experimental locations are 3.06 km away from the CORS station. The observational data are transmitted to the host computer and saved into a text file. The file name is automatically assigned as the name of the monitoring station, followed by the observation date. Table 3 shows a segment of simulated experimental observation data in the standard NMEA format. The observation data are then processed to detect and remove outliers and then converted to a local tangent plane coordinate system. Table 4 shows the coordinates of the monitoring points at different times after the removal of outliers.

Table 4: Coordinates of the monitoring point at different times in a time series after the removal of outliers

No	Time (UTC)	Geocentric Cartesian coordinates			Local tangent plane coordinates		
		X(m)	Y(m)	Z(m)	N(m)	E(m)	U(m)
1	04:59:37	-1768531.139	5688654.788	2270997.668	0.000	0.000	0.000
2	04:59:42	-1768531.141	5688654.795	2270997.672	-0.001	0.000	-0.008
3	04:59:47	-1768531.143	5688654.803	2270997.674	0.000	0.001	-0.016
4	04:59:52	-1768531.143	5688654.798	2270997.672	0.000	-0.001	-0.011
5	04:59:57	-1768531.142	5688654.800	2270997.674	-0.002	0.001	-0.013
6	05:00:02	-1768531.141	5688654.798	2270997.671	0.001	0.001	-0.010
7	05:00:07	-1768531.142	5688654.798	2270997.672	0.000	0.000	-0.011
8	05:00:12	-1768531.144	5688654.799	2270997.672	0.001	-0.001	-0.012
9	05:00:17	-1768531.144	5688654.801	2270997.675	-0.001	-0.001	-0.015
10	05:00:22	-1768531.146	5688654.805	2270997.675	0.000	-0.001	-0.013
…	….	……..	……..	…….	…….	…….	…….

Based on the coordinates of the observation time series, the observed horizontal and vertical displacements at simulation experiments location are detected, as shown in Table 5.

Table 5: Results of horizontal and vertical displacements observed from the simulation experiment

Campaign	Actual displacement (mm)		Observed displacement(mm)		Difference (mm)	
	Horizontal	Vertical	Horizontal	Vertical	Horizontal	Vertical
1	45	35	47.3	39.0	2.3	4.0
2	50	45	51.5	49.2	1.5	4.2
3	55	55	53.2	58.5	1.8	3.5
4	60	65	57.8	68.7	2.2	3.7

4.2. field experimental results.

Using the monitoring system that has been studied and developed, the monitoring experiments are conducted at the high-rise apartment building in Bac Tu Liem District, Hanoi City, Vietnam. The building has 24 storeys, 2 basements and 3 floors of commercial services. On the roof of the building, there are 04 corner observation stations with 4 monitoring station numbered Rover-01, Rover-02, Rover-03, and Rover-04 (Figure 12)

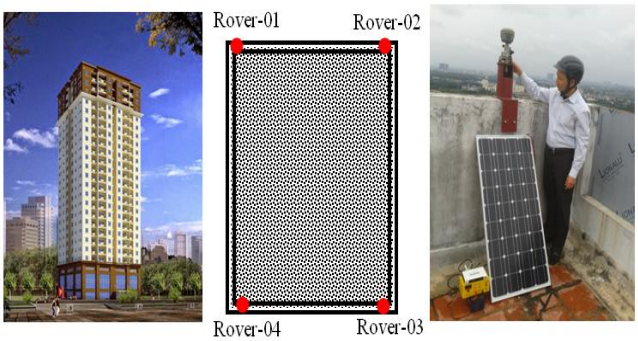

Figure 12 : Experimental monitoring of high-rise buildings CORS station named CORS-N001 used for monitoring is built on the campus of Hanoi University of Mining and Geology

and is about 2km from the high-rise apartment building (Figurre 13).

After installing monitoring stations on the roof of the building, monitoring is automatically performed. Data at the monitoring stations were continuously sent to the server in the NMEA standard format every second. The data is saved to the server by the default path and file name. The data of each day is saved to a file, the measurement message collected at the monitoring station and is sent to the NMEA-0183 standard format. Table 6 shows a piece of data collected at high-rise apartment building monitoring station.

Figure 13 : CORS N001 station system at Hanoi University of Mining and Geology

Table 6: A section of monitoring data of high-rise apartment building

$GPGGA,170000.000,2104.4617281,N,10545.8333509,E,4,13,0.8,10.451,M,-24.900,M,,0000*4C
$GPGLL,2104.4617281,N,10545.8333509,E,170000.000,A,R*46
$GPGSA,A,3,27,07,23,09,11,18,08,,,,,,1.8,0.8,1.6*3F
$GLGSA,A,3,78,77,88,87,81,68,,,,,,,1.8,0.8,1.6*2F
$GPGSV,4,1,14,08,79,009,55,41,54,229,50,23,51,222,51,09,50,267,52*75
$GPGSV,4,2,14,27,46,033,49,11,41,179,48,42,40,114,44,18,32,151,46*7F
$GPGSV,4,3,14,07,29,326,35,04,28,036,26,16,20,050,,01,16,174,26*79
$GPGSV,4,4,14,26,04,070,,28,03,267,*71 $GLGSV,3,1,09,88,66,146,45,87,47,044,47,77,40,039,38,78,27,338,42*62
$GLGSV,3,1,09,88,66,146,45,87,47,044,47,77,40,039,38,78,27,338,42*62
$GLGSV,3,2,09,81,24,190,42,67,17,229,30,68,17,284,40,76,10,097,23*6C
$GLGSV,3,3,09,79,01,310,*51
$GPVTG,000.00,T,,M,000.00,N,000.00,K,R*2E
$GPZDA,170000.000,31,10,2018,00,00*58
$GPGST,170000.000,0.005,0.003,0.002,86.5,0.002,0.003,0.004*5B
…… ……..

Results of processing of monitored data are implemented by home- made software and are presented in Table 7.

Table 7. Results processing of monitored data of high-rise apartment building

No	B o ′ ″	L o ′ ″	H (m)	X (m)	Y (m)	h (m)
1	21 4 11.158440	105 46 38.154462	68.407	2330873.187	580572.482	93.469
2	21 4 11.158470	105 46 38.154516	68.410	2330873.188	580572.484	93.472
3	21 4 11.158440	105 46 38.154558	68.409	2330873.187	580572.485	93.471
4	21 4 11.158554	105 46 38.154456	68.402	2330873.190	580572.482	93.464
5	21 4 11.158434	105 46 38.154552	68.405	2330873.186	580572.485	93.467
6	21 4 11.158530	105 46 38.154486	68.409	2330873.189	580572.483	93.471
7	21 4 11.158554	105 46 38.154522	68.410	2330873.190	580572.484	93.472
8	21 4 11.158440	105 46 38.154468	68.402	2330873.187	580572.482	93.464
9	21 4 11.158422	105 46 38.154492	68.405	2330873.186	580572.483	93.467
10	21 4 11.158464	105 46 38.154450	68.407	2330873.187	580572.482	93.469
11	21 4 11.158482	105 46 38.154564	68.402	2330873.188	580572.485	93.464
12	21 4 11.158428	105 46 38.154528	68.405	2330873.186	580572.484	93.467
13	21 4 11.158566	105 46 38.154450	68.407	2330873.190	580572.482	93.469
14	21 4 11.158566	105 46 38.154510	68.402	2330873.190	580572.484	93.464
15	21 4 11.158494	105 46 38.154504	68.405	2330873.188	580572.483	93.467
16	21 4 11.158518	105 46 38.154450	68.402	2330873.189	580572.482	93.464
17	21 4 11.158536	105 46 38.154444	68.402	2330873.190	580572.482	93.464
18	21 4 11.158554	105 46 38.154420	68.403	2330873.190	580572.481	93.465
19	21 4 11.158452	105 46 38.154564	68.410	2330873.187	580572.485	93.472
20	21 4 11.158464	105 46 38.154516	68.401	2330873.187	580572.484	93.463
...	.....	.....	.....	.....	.....	.....

After processing and determining the coordinates of monitoring station the average of daily coordinates value for a project, and from there calculated the displacement value of the project.

4.3 Discussions

In displacement simulated experiments, the observations were conducted at survey station locations with varying baseline distances is 3.06km, the largest differences between the actual and observed displacements were 2.3 mm in the horizontal direction and 4.2 mm in the vertical direction.

This difference is quite small, so this monitoring system is suitable for displacement monitoring of works such as high-rise buildings, dams and bridges.

5. Conclusion

This research successfully demonstrates the development of a real-time displacement monitoring system utilizing GNSS/CORS technology. The system integrates cost-effective hardware with reliable data transmission and processing algorithms, providing high-precision results validated through both simulation and field testing. The

observed displacement measurements closely matched actual values, indicating strong reliability. This system offers a scalable and efficient solution for continuous monitoring of infrastructure, particularly high-rise buildings, bridges, and dams.

References

[1] N. Quesada-Olmo, M.J. Jimenez-Martinez, M. Farjas-Abadia, 2018. Real-time high-rise building monitoring system using global navigation satellite system technology. Journal of Measurement, 123, 115-124.
[2] Wan Abdul Aziz Wan Mohd Akib, Shu Kian Kok Zulkarnaini Mat Amin, 2012. High Rise Building Deformation Monitoring With GPS. Department of Geomatic Engineering Faculty of Geoinformation Science & Engineering University Teknologi Malaysia, 81310 Skudai, Johor Malaysia.
[3] Ruijie Xi, Weiping Jiang, Xiaolin Meng, Hua Chen, Qusen Chen, 2018. Bridge monitoring using BDS-RTK and GPS-RTK techniques, Journal of Measurement, 120, 128-139.
[4] Bochen Zhang, Xiaoli Ding, Charles Werner, Kai Tan, Bin Zhang, Mi Jiang, Jingwen Zhao, Youlin Xu, (2018). Dynamic displacement monitoring of long-span bridges with a microwave radar interferometer. ISPRS Journal of Photogrammetry and Remote Sensing, 138, p252-264.
[5] National Marine Electronics Association (NMEA); https://www.nmea.org/
[6] Networked Transport of RTCM via Internet Protocol (Ntrip), Version 1.0. In: *GDC (GNSS Data Center)* [online]. Bundesamt für Kartographie und Geodäsie (BKG), 2004. [cit.26.05.2016]. Available from:http://igs.bkg.bund.de/root_ftp/NTRIP/documentation/NtripDocumentation.pdf/.
[7] Pengxu Wang, Hui Liu, Guigen Nie, Zhixin Yang, Jiaji Wu, Chuang Qian, Bao Shu (2022). Performance evaluation of a real-time high-precision landslide displacement detection algorithm based on GNSS virtual reference station technology. Measurement 199 (2022) 111457. https://doi.org/10.1016/j.measurement.2022.111457.
[8] https://globalgpssystems.com/wp-content/uploads/2020/09/net_s9.pdf
[9] https://oemgnss.trimble.com/en/products/receiver-modules/bd970
[10] Nan Shen, Liang Chen, Ruizhi Chen (2022). Displacement detection based on Bayesian inference from GNSS kinematic positioning for deformation monitoring. Mechanical Systems and Signal Processing 167 (2022) 108570. https://doi.org/10.1016/j.ymssp.2021.108570.
[11] Ali Shehadeh, Odey Alshboul, Ghassan Almasabha. Slope displacement detection in construction: An automated management algorithm for disaster prevention. Expert Systems with Applications 237 (2024) 121505. https://doi.org/10.1016/j.eswa.2023.121505.